Article

Adverse Outcome Following Mild Traumatic Brain Injury Is Associated with Microstructure Alterations at the Gray and White Matter Boundary

Lara Pankatz [1,2,†], Philine Rojczyk [1,2,†], Johanna Seitz-Holland [1,3], Sylvain Bouix [1,4], Leonard B. Jung [1,2], Tim L. T. Wiegand [1,2], Elena M. Bonke [1,2,5], Nico Sollmann [1,2,6,7,8], Elisabeth Kaufmann [1,2,9], Holly Carrington [1,10], Twishi Puri [1], Yogesh Rathi [1], Michael J. Coleman [1], Ofer Pasternak [1,11], Mark S. George [12,13], Thomas W. McAllister [14], Ross Zafonte [15,16], Murray B. Stein [17,18,19], Christine E. Marx [20,21], Martha E. Shenton [1,11] and Inga K. Koerte [1,2,3,5,*]

1 Psychiatry Neuroimaging Laboratory, Department of Psychiatry, Brigham and Women's Hospital, Harvard Medical School, Somerville, MA 02145, USA; lara.pankatz@med.uni-muenchen.de (L.P.); philine.rojczyk@med.uni-muenchen.de (P.R.); jseitz@bwh.harvard.edu (J.S.-H.); sylvain.bouix@etsmtl.ca (S.B.); leonard.jung@med.uni-muenchen.de (L.B.J.); tim.wiegand@med.uni-muenchen.de (T.L.T.W.); elena.bonke@med.uni-muenchen.de (E.M.B.); nico.sollmann@tum.de (N.S.); elisabeth.kaufmann@med.uni-muenchen.de (E.K.); holly.carrington@mountsinai.org (H.C.); tpuri1@bwh.harvard.edu (T.P.); yogesh@bwh.harvard.edu (Y.R.); mjc@bwh.harvard.edu (M.J.C.); ofer@bwh.harvard.edu (O.P.); shenton@bwh.harvard.edu (M.E.S.)
2 cBRAIN, Department of Child and Adolescent Psychiatry, Psychosomatic and Psychotherapy, Ludwig-Maximilians-Universität, 80336 Munich, Germany
3 Department of Psychiatry, Massachusetts General Hospital, Harvard Medical School, Boston, MA 02114, USA
4 Département de génie logiciel et TI, École de Technologie Supérieure, Université du Québec, Montreal, QC H3C 1K3, Canada
5 Graduate School of Systemic Neuroscience, Ludwig-Maximilians-Universität, 82152 Planegg, Germany
6 Department of Diagnostic and Interventional Radiology, University Hospital Ulm, 89081 Ulm, Germany
7 Department of Diagnostic and Interventional Neuroradiology, School of Medicine, Klinikum rechts der Isar, Technical University of Munich, 81675 Munich, Germany
8 TUM-Neuroimaging Center, Klinikum rechts der Isar, Technical University of Munich, 81675 Munich, Germany
9 Department of Neurology, University Hospital, LMU, 81377 Munich, Germany
10 Brain Injury Research Center of Mount Sinai, Icahn School of Medicine at Mount Sinai, New York, NY 10029, USA
11 Department of Radiology, Brigham and Women's Hospital, Harvard Medical School, Boston, MA 02115, USA
12 Psychiatry Department, Medical University of South Carolina, Charleston, SC 29425, USA; georgem@musc.edu
13 Ralph H. Johnson VA Medical Center, Charleston, SC 29401, USA
14 Department of Psychiatry, Indiana University School of Medicine, Indianapolis, IN 46202, USA; twmcalli@iupui.edu
15 Department of Physical Medicine and Rehabilitation, Spaulding Rehabilitation Hospital, Harvard Medical School, Charlestown, MA 02129, USA; rzafonte@partners.org
16 Department of Physical Medicine and Rehabilitation, Brigham and Women's Hospital, Harvard Medical School, Boston, MA 02115, USA
17 Department of Psychiatry, University of California San Diego, La Jolla, CA 92093, USA; mstein@ucsd.edu
18 School of Public Health, University of California San Diego, La Jolla, CA 92093, USA
19 Psychiatry Service, VA San Diego Healthcare System, San Diego, CA 92161, USA
20 VA Mid-Atlantic Mental Illness Research and Clinical Center (MIRECC) and Durham VA Medical Center, Durham, NC 27705, USA; christine.marx@duke.edu
21 Department of Psychiatry and Behavior Sciences, Duke University School of Medicine, Durham, NC 27710, USA
* Correspondence: ikoerte@med.lmu.de; Tel.: +49-4400-56903
† These authors contributed equally to this work.

Abstract: The gray matter/white matter (GM/WM) boundary of the brain is vulnerable to shear strain associated with mild traumatic brain injury (mTBI). It is, however, unknown whether GM/WM microstructure is associated with long-term outcomes following mTBI. The diffusion and structural MRI data of 278 participants between 18 and 65 years of age with and without military background from the Department of Defense INTRuST study were analyzed. Fractional anisotropy (FA) was

extracted at the GM/WM boundary across the brain and for each lobe. Additionally, two conventional analytic approaches were used: whole-brain deep WM FA (TBSS) and whole-brain cortical thickness (FreeSurfer). ANCOVAs were applied to assess differences between the mTBI cohort (n = 147) and the comparison cohort (n = 131). Associations between imaging features and post-concussive symptom severity, and functional and cognitive impairment were investigated using partial correlations while controlling for mental health comorbidities that are particularly common among military cohorts and were present in both the mTBI and comparison group. Findings revealed significantly lower whole-brain and lobe-specific GM/WM boundary FA ($p < 0.011$), and deep WM FA ($p = 0.001$) in the mTBI cohort. Whole-brain and lobe-specific GM/WM boundary FA was significantly negatively correlated with post-concussive symptoms ($p < 0.039$), functional ($p < 0.016$), and cognitive impairment ($p < 0.049$). Deep WM FA was associated with functional impairment ($p = 0.002$). Finally, no significant difference was observed in cortical thickness, nor between cortical thickness and outcome ($p > 0.05$). Findings from this study suggest that microstructural alterations at the GM/WM boundary may be sensitive markers of adverse long-term outcomes following mTBI.

1. Introduction

Traumatic brain injury (TBI) is a leading cause of disability and is particularly common among military service members [1,2]. About 90% of TBI cases are categorized as mild TBI (mTBI) and affect as many as ~42 million people annually worldwide [3,4]. About a third of individuals with mTBI will go on to develop long-term symptoms, also referred to as persistent post-concussive symptoms [5]. Nonetheless, and despite the high prevalence of mTBI and the large number of individuals with adverse long-term outcomes, the underlying pathophysiology is still not fully understood.

The current understanding is that during a head impact, rotational and linear forces act on the skull, leading to brain tissue deformation and, thereby the stretching and shearing of axons [6]. The latter may result in microinjury of axons, also known as traumatic axonal injury (TAI), which is one of the most common injuries associated with mTBI [7]. The gray matter/white matter (GM/WM) boundary is particularly susceptible to TAI, given that WM is more rigid and viscous than GM and reacts less rapidly to mechanical strain, potentially leading to the shearing of the two types of tissues juxtaposed to one another [8,9]. Indeed, recent computer simulations suggest that the GM/WM boundary is where acceleration and shear forces are at their highest levels [10]. Moreover, microbleeds, which constitute a prevalent pathophysiologic feature of brain tissue strain are commonly found along the GM/WM boundary [11]. Of note, WM microinjuries to the brain tissue have previously been associated with the development of long-term post-concussive symptoms [12]. These symptoms may involve cognitive and functional disability including compromised processing speed, executive functioning, and problems with participation in social activities, work, and family life [13].

Strikingly, microinjuries to WM often remain undetected by conventional imaging modalities (e.g., computed tomography (CT)) and thus their detection requires the use of more sensitive advanced imaging techniques. Importantly, diffusion magnetic resonance imaging (dMRI) can both detect and quantify even subtle alterations in brain structure. Specifically, dMRI measures the magnitude and orientation of water molecule diffusion in brain tissue, expressed as fractional anisotropy (FA) [14].

Previous studies investigating individuals with a history of mTBI have focused on brain alterations of either the most central part of WM ("deep WM") [15,16] or GM [17,18]. Interestingly, these studies revealed variable findings, with some reporting increases or decreases in FA in the chronic phase following mTBI [15], while others did not observe differences in FA between mTBI individuals and a comparison group [16]. Similarly, when

assessing GM structure following mTBI, some studies report alterations in GM cortical thickness [17], while other studies do not reveal any differences in GM compared to controls [18] in the acute and sub-acute stages after mTBI. Conflicting results have further been reported in the chronic stages, where some studies describe thinning of the cortex [19], while others report thickening in the same GM regions [20]. In fact, time since injury is an important aspect when considering brain structural alterations following mTBI. Some studies have suggested that even in the case that rehabilitative processes lead to presumed recovery after a couple of weeks or months, degenerative processes may commence later in life and may be linked to disadvantageous outcomes, such as accelerated aging and declining cognitive functioning [21,22]. It is possible that previous studies did not observe alterations in brain microstructure following mTBI because they failed to assess what may constitute the most vulnerable region of injury, and that is the GM/WM boundary. This may also explain why some individuals with mTBI exhibit post-concussive symptoms despite any visible signs of tissue alteration in either the deep WM [23] or the cortex [24].

The aim of this study is to characterize the microstructure at the GM/WM boundary in participants of the Department of Defense Injury and Traumatic Stress (INTRuST) study with a history of mTBI against a comparison group while adjusting for common confounders of brain structure such as age, gender, post-traumatic stress disorder (PTSD), depressive symptoms, and alcohol use. In addition, we investigate whether alterations in GM/WM boundary diffusion properties are associated with clinical outcome measures following mTBI, including post-concussive symptom severity, cognitive functioning, and functional impairment. Finally, since this is the first investigation focusing on the GM/WM boundary in this population, we also apply more commonly used approaches to investigate brain structure following mTBI (i.e., WM diffusion of the deep WM and cortical thickness).

2. Materials and Methods

2.1. Study Design and Participants

Participants of the Injury and Traumatic Stress (INTRuST) Clinical Consortium (Department of Defense, W81XWH-08-2-0159, intrust.sdsc.edu, accessed on 6 January 2022) were enrolled from 10 sites across the United States between 2008 and 2013. Institutional review board study approval was obtained from all participating sites and the study was conducted in conformity with the Declaration of Helsinki. All study participants provided written informed consent prior to enrolment.

Participants included English-speaking males or females between the ages of 18 and 70 years of age. Participants were excluded from the study if they had acquired English as a second language after the age of 5, had a history of a learning disability, a TBI history that resulted in a hospital stay and/or abnormal imaging findings, a history of moderate to severe TBI, a diagnosis of Bipolar I, psychotic, delirious, or dementia-related disorders, uncontrolled chronic disease, uncontrolled hypertension, or were taking more than one antihypertensive medication, used oral or intramuscular steroids within the past four months, or were currently taking drugs or any medication affecting brain function (other than psychotropic medication). Individuals with a history of psychotropic drug, alcohol, or substance use were permitted to participate in the study if they had been in remission for the last 30 days prior to data collection. Additional exclusion criteria were general MRI contraindications, disorders of the central nervous system, or pregnancy/lactating.

Out of the 771 enrolled participants, 373 completed neuropsychological and MRI assessments. After the evaluation of MRI data quality, 95 cases were excluded due to severe motion artifacts (*n* = 14), harmonization issues (*n* = 44), or missing demographic data (*n* = 37) leaving a total of 278 participants with available structural and dMRI data. The enrolled participants did not differ significantly from those excluded in any demographic variable (*p* > 0.05). These participants were classified into participants with a history of mTBI (*n* = 147) and a comparison group without mTBI (*n* = 131) (Table 1). Participants with psychiatric comorbidities (other than severe mental disorders such as schizophrenia and bipolar disorder) were not excluded from either group given that we aimed for a most

accurate resemblance of the larger population, and psychiatric symptoms are common in the military population and those with mTBI.

Table 1. Sample Characteristics.

		Total Sample		mTBI		No mTBI		ANCOVA	
Demographics		*n*	mean ± SD	*n*	mean ± SD	*n*	mean ± SD	*F*(df)	*p*
Age		278	36.27 ± 12.71	147	36.56 ± 11.97	131	34.62 ± 12.88	1.70(1, 276)	0.193
Years between injury and scan		-	-	101	7.57 ± 9.54	-	-	-	-
								Fisher's exact test	
			%		%		%	χ^2	*p*
Gender (male/female)			54.3/45.7		65.3/34.7		41.9/58.1	15.31	<0.001
Race	Native		0.7		1.4		-	13.74	0.193
	Asian		3.2		1.4		5.3		
	Pacific		0.4		-		0.8		
	African American		13.7		10.2		17.6		
	White		76.3		82.9		68.7		
	Unknown		5.7		4.1		7.6		
								ANCOVA	
Imaging		*n*	mean ± SD	*n*	mean ± SD	*n*	mean ± SD	*F*(df)	*p (pFDR)*
Whole-brain GM/WM Boundary FA		278	0.27 ± 0.02	147	0.27 ± 0.02	131	0.28 ± 0.01	23.16(1, 271)	**<0.001 (0.001)**
Frontal lobe GM/WM Boundary FA		278	0.28 ± 0.02	147	0.28 ± 0.02	131	0.29 ± 0.02	18.62(1, 271)	**<0.001 (0.001)**
Parietal lobe GM/WM Boundary FA		278	0.27 ± 0.04	147	0.26 ± 0.05	131	0.28 ± 0.03	8.88(1, 271)	**0.003 (0.004)**
Temporal lobe GM/WM Boundary FA		278	0.28 ± 0.02	147	0.27 ± 0.02	131	0.28 ± 0.01	27.78(1, 271)	**<0.001 (0.001)**
Occipital lobe GM/WM Boundary FA		278	0.25 ± 0.02	147	0.25 ± 0.02	131	0.26 ± 0.02	6.65(1, 271)	**0.010 (0.011)**
Deep white matter FA		278	0.58 ± 0.02	147	0.57 ± 0.02	131	0.59 ± 0.02	25.21(1, 271)	**<0.001 (0.001)**
Whole-brain cortical thickness		278	2.37 ± 0.09	147	2.35 ± 0.08	131	2.37 ± 0.10	0.039(1, 271)	0.843 (0.843)
Psychiatric Symptoms								*F*(df)	*p*
PCL-C		278	30.40 ± 17.58	147	36.66 ± 18.50	131	23.30 ± 13.38	35.35(1, 274)	**<0.001**
PHQ-9		278	4.40 ± 5.67	147	6.61 ± 5.99	131	1.92 ± 4.06	47.72(1, 274)	**<0.001**
Alcohol Use									
AUDIT-10		278	3.73 ± 5.50	147	4.67 ± 6.40	131	2.67 ± 4.03	6.63(1, 274)	**0.011**
Post-Concussive Symptoms									
RPQ13		168	13.25 ± 15.04	139	17.35 ± 14.79	29	3.76 ± 11.23	21.83(1, 166)	**<0.001**
Functional Impairment									
SDS		275	6.36 ± 9.07	147	10.44 ± 9.70	128	1.67 ± 5.28	74.47(1, 271)	**<0.001**
Cognitive Functioning								*F*(df)	*p*
TMT-A time (seconds)		275	24.92 ± 10.21	145	26.58 ± 10.78	130	23.06 ± 9.24	6.10(1,271)	**0.014**
TMT-B time (seconds)		275	55.65 ± 27.52	145	58.19 ± 27.52	130	52.84 ± 26.83	0.89(1,271)	0.348

Note. SD, Standard deviation; PCL-C, PTSD Checklist Civilian; PHQ-9, Patient Health Questionnaire; SDS, Sheehan Disability Scale; AUDIT, Alcohol Use Disorder Identification Test, RPQ13, Rivermead Post-Concussion Questionnaires 13; All ANCOVAs were corrected for age and gender. Imaging parameters were corrected for age, gender, PCL-C, PHQ-9, and AUDIT-10. Significant *p*-values are marked in bold font.

2.2. Diagnostic and Clinical Assessments

2.2.1. Assessment of mTBI

Mild TBI history was assessed using the self-report INTRuST mTBI Screening Instrument which closely follows the American Congress of Rehabilitation Medicine's diagnostic guidelines [25] and has been used in previous publications of the INTRuST Clinical Consortium [26]. MTBI was diagnosed if a head injury led to any of the following: alteration or loss of consciousness and/or posttraumatic anterograde/retrograde amnesia.

2.2.2. Assessment of Post-Concussion Symptom Severity

The Rivermead Post-Concussion Symptoms Questionnaire (RPQ13) [27] is an established scale for assessing chronic persistent post-concussive symptoms with strong internal validity, test–retest reliability, and inter-rater reliability [28]. Higher scores on the RPQ13 indicate greater post-concussive symptom severity.

2.2.3. Assessment of Functional Impairment

To assess functional impairment, the Sheehan Disability Scale (SDS) was employed [29]. The SDS is a self-report questionnaire that includes three items that assess functional impairment in daily work, social, and family life (e.g., "symptoms have disrupted family/home responsibilities"). The scale is rated from 0 ("not at all") to 10 ("extreme"). This scale was used to assess functional impairment in daily work, social, and family life. Higher scores on the SDS indicate greater functional impairment.

2.2.4. Assessment of Cognitive Functioning

The Trail Making Test (TMT) [30] is a highly efficient tool to assess cognitive functioning, such as processing speed (TMT-A) and executive functioning, including mental flexibility and task switching, attention, and visual tracking (TMT-B). TMT-A assesses how fast a participant can connect 25 numbers in ascending order (i.e., 1-2-3 etc.) that are randomly arranged on a sheet of paper. TMT-B requires the participant to alternate between connecting letters and numbers in numerical and alphabetical order, respectively (i.e., 1-A-2-B etc.). For both TMT-A and B, the total time to completion is assessed. The TMT is sensitive in discriminating between individuals with brain alterations and healthy controls [31].

2.2.5. Assessment of Psychiatric Comorbidities

The presence and severity of PTSD symptoms were assessed using the PTSD Checklist-Civilian Version (PCL-C) [32], a 17-item self-report questionnaire corresponding to the Diagnostic and Statistical Manual of Mental Disorders IV (DSM-IV) diagnostic criteria for PTSD. Items (e.g., "repeated, disturbing memories, thoughts, or images of a stressful experience from the past?") are rated on a scale from 1 "not at all bothersome" to 5 "extremely bothersome," and summed into a total symptom severity score.

The severity of depressive symptoms was assessed using the 9-Item Patient Health Questionnaire 9 (PHQ-9), with items rated from 0 "not at all" to 3 "nearly every day" [33]. A total symptom severity score was computed by summing all items.

The Alcohol Use Disorders Identification Test (AUDIT-10) was used to assess alcohol consumption [34]. The AUDIT-10 consists of 10 items that cover the quantity of alcohol consumed, level of dependency, and harmful consequences for self and others. Items (e.g., "How many drinks containing alcohol do you have on a typical day when you are drinking?") are scored on a scale from 0 to 4 with varying response options depending on the question. A total alcohol use severity score was computed by summing all items. Higher scores correspond to greater alcohol use severity.

2.3. MRI Acquisition and Image Processing

2.3.1. Image Acquisition

Structural MRI sequences and dMRI sequences were acquired on 3-Tesla scanners (Tim Trio, Siemens Healthineers, Erlangen, Germany; GE 750, GE Healthcare, Chicago, IL, USA, or Achieva, Philips Healthcare, Best, The Netherlands) across six out of ten INTRuST study sites (for details for each MRI system, see Table 2).

Table 2. Acquisition parameters for MRI.

Sequence	Parameter	SIEMENS	PHILIPS	GE
DTI				
	Orientation	axial	axial	axial
	Phase Encoding Direction	a/p	p/a	l/r
	FOV (in mm)	256	256	256
	Bandwidth (in kHz or Hz/Px)	1396	1271	250
	Number of Directions	87	64	86
	b-value	900	900	900

Table 2. *Cont.*

Sequence	Parameter	SIEMENS	PHILIPS	GE
	Number of b0	0	7	1
	Resolution Matrix	128 × 128	128 × 128	128 × 128
	Voxel Size (in mm^3)	2 × 2 × 2	2 × 2 × 2	2 × 2 × 2
	Number of Slices	73	73	73
	Acquisition Time (in min)	14:08	14:21	14:40
T1w				
	Sequence details	MP-RAGE	T1W_3D_TFE SENSE	SPGR-BRAVO
	Orientation	Sagittal	Sagittal	Sagittal
	Flip Angle (in degrees)	7	7	10
	FOV (in mm)	256	256	256
	Bandwidth (in kHz)	25.6	24.5	25.0
	TE (in ms)	3.3	3.5	3.7
	TR (in ms)	2530	7600	9150
	Inversion Time	1100	1100	600
	Resolution Matrix	256 × 256	256 × 256	256 × 256
	Voxel Size (in mm^3)	1 × 1 × 1	1 × 1 × 1	1 × 1 × 1
	Number of Slices	176	176	176
	Acquisition Time (in min)	6:03	5:13	5:15

Note. Multi-site study; MRI data acquisition on Tim Trio, Siemens Healthineers, Erlangen, Germany; GE 750, GE Healthcare, Chicago, IL, USA; Achieva, Philips Healthcare, Best, The Netherlands. FOV, Field of view; TE, Echo time; TR, Repetition time.

2.3.2. Image Pre-Processing

Pre-processing of the structural and dMRI images was conducted according to the in-house pipeline of the Psychiatry Neuroimaging Laboratory, Brigham and Women's Hospital, Harvard Medical School (https://github.com/pnlbwh/pnlNipype, accessed on 10 December 2021). This included axis alignment, centering, and motion correction of all images. For the dMRI images, eddy current correction was applied. The image quality was visually inspected and semi-automatically examined for artifacts (e.g., motion artifacts) using 3D Slicer (version 4.5, Surgical Planning Laboratory, Brigham and Women's Hospital, Boston, MA, USA; http://www.slicer.org, accessed on 10 December 2021) [35]. Structural and diffusion masks covering the entire brain were constructed and manually corrected in 3D Slicer where necessary (e.g., in case of incomplete coverage of the brain) by a trained rater.

2.3.3. Structural Image Processing

To accurately delineate the GM/WM boundary, FreeSurfer was used (version 5.3, Laboratory for Computational Neuroimaging, Boston, MA, USA; https://surfer.nmr.mgh.harvard.edu, accessed 15 January 2022) [36]. Processing of the structural data included the removal of non-brain tissue, automated Talairach transformation, grayscale intensity normalization, correction for any inhomogeneities in the magnetic field, automated topology correction, and surface deformation correction referring to intensity gradients. Subsequent steps included surface inflation, registration to a common spherical atlas, and parcellation of the cortex into 150 regions of interest (ROIs, 75 per hemisphere) according to the Destrieux brain atlas [37]. This resulted in a 3D reconstruction of the GM/WM boundary, which was visually quality checked to ensure anatomical accuracy.

To account for alterations in the GM, cortical thickness was calculated as the distance between the GM/WM boundary (i.e., white surface) and the GM/cerebrospinal fluid (CSF) boundary (i.e., pial surface) [38]. Measurements of cortical thickness were smoothed using a standard Gaussian kernel to enhance contrast.

2.3.4. Diffusion-Weighted Image Processing

Given the multi-site nature of the INTRuST project and the associated scanner variability, an established single-shell harmonization algorithm (https://github.com/pnlbwh/dMRIharmonization, accessed 10 January 2022) was used on the b = 900 dMRI data to account for scanner differences, while maintaining within-site inter-subject variability [39]. Using a least-squares fit model to derive diffusion tensors from the preprocessed diffusion-weighted images, voxel-based FA maps were produced. FA is a diffusion metric that ranges between 0 (*isotropic*, unrestricted diffusion) and 1 (*anisotropic*, restricted diffusion) and expresses the magnitude and direction of water molecule diffusion in the tissue [40]. Additionally, free-water (FW) imaging was used to estimate and eliminate the relative contribution of extracellular FW (e.g., due to CSF, edema, or atrophy) [41]. After accounting for FW, corrected FA maps were extracted.

Deep WM was examined using tract-based spatial statistics (TBSS; https://github.com/pnlbwh/TBSS, accessed 26 January 2022) [42], according to the Enhancing Neuro Imaging Genetics by Meta-Analysis Diffusion Tensor Imaging (ENIGMA-DTI) working group's protocol (http://enigma.ini.usc.edu/ongoing/dti-working-group/, accessed 26 January 2022). The FA maps generated were co-registered onto the ENIGMA-DTI template and subsequently projected onto the ENIGMA-DTI skeleton [43]. A skeletonized FA map was produced, depicting the core of each participant's WM fiber pathways. Last, average FW-corrected FA values were extracted from each participant's FA skeleton.

2.3.5. Registration and Extraction of Diffusion Metrics at the GM/WM Boundary

To estimate FA values along the GM/WM boundary, we registered the b = 0 map from the dMRI scan to the Freesurfer subject's space using boundary-based registration [10,44] (FS command: bbregister, option –t2 to indicate the b = 0 contrast is similar to a T2 weighted image). The resulting transformation was then used to co-register and map the subject's FA image (in original dMRI space) to the Freesurfer "white" left and right hemisphere surfaces (FS command: mri_vol2surf) (Figure 1). We then extracted FA values for the GM/WM boundary across the brain (whole-brain), as well as for each of the major brain lobes, frontal, parietal, temporal, and occipital lobe according to the Destrieux brain atlas [37]. When merging ROIs, the average FA of the merged region was computed via a weighted sum of the mean FA of the individual ROIs to account for area differences between individual ROIs.

2.4. Statistical Analysis

SPSS software (version 25.0; IBM Statistics for Mac, Armonk, NY, USA) was used for all statistical analyses. Age, gender, PTSD symptoms (PCL-C), depressive symptoms (PHQ-9), and alcohol use (AUDIT-10) were included as covariates in all models to account for potentially confounding effects on brain structure. Significance values were corrected for multiple comparisons according to the Benjamini–Hochberg method (false discovery rate (FDR)) [45]. *p*-values were adjusted for seven analyses referring to seven outcome measures (whole-brain, frontal, parietal, temporal, and occipital lobe GM/WM boundary FA, deep WM FA, and cortical thickness). An FDR-corrected *p*-value of 0.05 was set to indicate statistical significance.

2.4.1. Group Differences in GM/WM Boundary Diffusion, Deep WM Diffusion, and Cortical Thickness

We conducted seven analyses of covariance (ANCOVAs) to assess differences in whole-brain, frontal, parietal, temporal, and occipital lobe GM/WM boundary FA, deep WM FA, and cortical thickness (respective dependent variables) between groups of participants with mTBI compared to the comparison group without mTBI (independent variable).
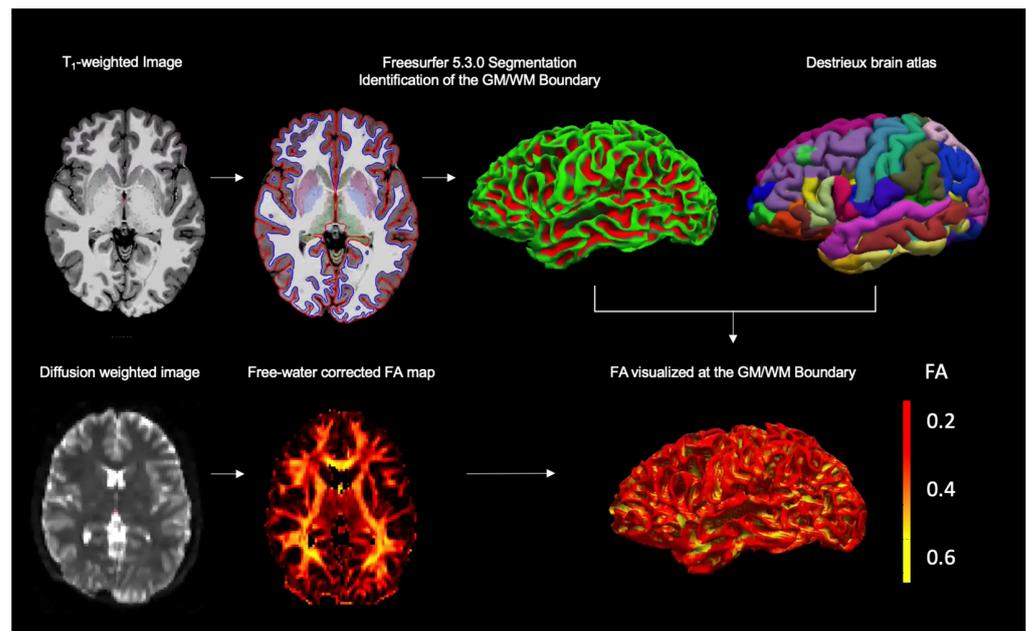
Figure 1. Image Processing. Structural MRI sequences were segmented into GM and WM using FreeSurfer 5.3.0, to identify the GM/WM boundary (in blue). Diffusion MRI (dMRI) images were fitted with the free-water (FW) map to create a voxel-wise map of FA corrected for FW. Each participant's FW-corrected dMRI data were registered onto the respective FreeSurfer segmentation. All images were overlaid with the Destrieux brain atlas to identify and extract FA values along the GM/WM intersection in different regions of the brain. *Note.* GM, gray matter; WM, white matter; FA, fractional anisotropy $_{\text{Tissue}}$; Images are displayed using Freeview. The FW-corrected FA map is shown in color scheme 'Heat' for better visualization.

2.4.2. Correlation between GM/WM Boundary Diffusion and Post-Concussive Symptoms, Functional Impairment, and Cognitive Functioning

To determine whether GM/WM boundary diffusion serves as an indicator of long-term outcome after mTBI, we assessed correlations between whole-brain, frontal, parietal, temporal, and occipital lobe GM/WM boundary FA, deep WM FA, cortical thickness, and chronic post-concussive symptoms (RPQ13), functional impairment (in work, social, and family life (SDS)), and cognitive functioning (processing speed (TMT-A) and executive functioning (TMT-B)). Nonparametric partial correlations were used due to non-normal distributions of the outcome variables.

The data presented in this study is available upon request from the corresponding author.

3. Results

The sample characteristics and of the study sample are presented in Table 1, together with summary statistics and analytical results. The age and racial distribution between the groups did not differ ($p > 0.05$). However, there was an unequal gender distribution between the two groups ($p < 0.001$). ANCOVA further revealed greater PTSD and depressive symptoms in the mTBI group ($p < 0.001$), as well as higher alcohol consumption ($p = 0.011$). Furthermore, the mTBI group displayed greater chronic post-concussive symptoms ($p = < 0.001$) and significantly greater functional impairment ($p = < 0.001$). The mTBI group showed worse processing speed than the comparison group ($p = 0.014$), however, there was no significant difference between the groups for executive functioning ($p = 0.348$).

3.1. Group Differences in GM/WM Boundary Diffusion, Deep WM Diffusion, and Cortical Thickness

The ANCOVAs revealed significant lower whole-brain ($p < 0.001$, pFDR = 0.001), frontal ($p < 0.001$, pFDR = 0.001), parietal ($p = 0.003$, pFDR = 0.004), temporal ($p < 0.001$, pFDR = 0.001), and occipital lobe ($p = 0.010$, pFDR = 0.011) GM/WM boundary FA and deep

WM FA (*p* < 0.001, pFDR = 0.001) in the mTBI compared to the no mTBI group. However, no significant differences were found for cortical thickness (*p* = 0.843, pFDR = 0.843) between the mTBI group and the no mTBI group. (Table 1, Figure 2).
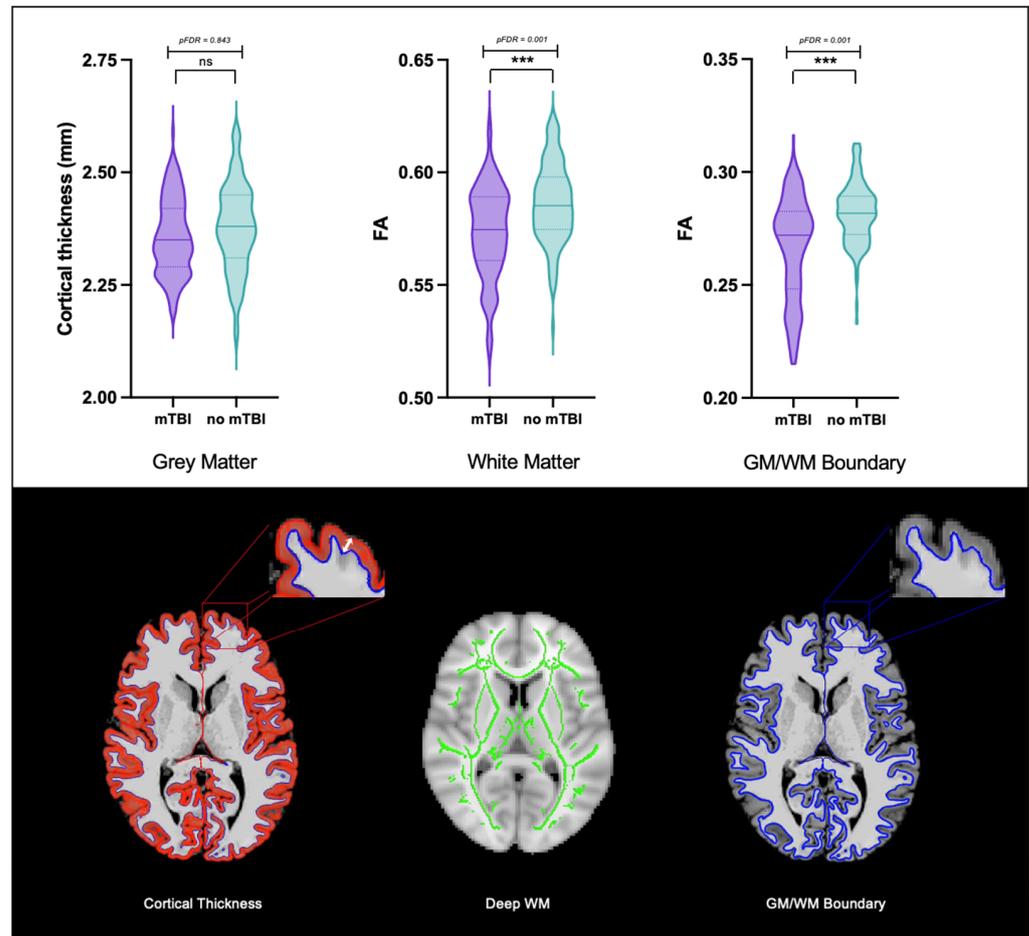

Figure 2. Group differences between participants with mTBI and participants without mTBI. ANCOVA revealed significantly lower whole-brain GM/WM boundary FA (pFDR = 0.001), and deep WM FA (pFDR = 0.001) in mTBI subjects compared to participants without mTBI. No significant differences were observed between groups in cortical thickness (pFDR = 0.843). The area of the brain where the imaging measure was acquired is displayed beneath for better visualization. *Note.* mTBI, Mild traumatic brain injury; FA, Fractional Anisotropy; ns = not significant; *** = *p* < 0.001.

3.2. Correlation between GM/WM Boundary Diffusion and Post-Concussive Symptoms, Functional Impairment, and Cognitive Functioning

Having more post-concussive symptoms (RPQ13) was significantly negatively correlated with lower whole-brain (r = −0.19, *p* = 0.017, pFDR = 0.039), frontal (r = −0.21, *p* = 0.007, pFDR = 0.024), and parietal (r = −0.21, *p* = 0.006, pFDR = 0.024) GM/WM boundary FA_T, but not with temporal (r = −0.16, *p* = 0.043, pFDR = 0.075) and occipital GM/WM boundary FA_T (r = 0.06, *p* = 0.404, pFDR = 0.404), deep WM FA_T (r = −0.12, *p* = 0.117, pFDR = 0.163), or cortical thickness (r = 0.10, *p* = 0.201, pFDR = 0.234).

The analyses further revealed significant associations between functional impairment (SDS) and lower whole-brain (r = −0.23, *p* < 0.001, pFDR = 0.002), frontal (r = −0.19, *p* = 0.001, pFDR = 0.002), parietal (r = −0.17, *p* = 0.004, pFDR = 0.006), temporal (r = −0.25, *p* = < 0.001, pFDR = 0.002), and occipital (r = −0.15, *p* = 0.014, pFDR = 0.016) GM/WM boundary FA_T as well as deep WM FA_T (r = 0.25, *p* < 0.001, pFDR = 0.002), but not for cortical thickness (r = −0.05, *p* = 0.413, pFDR = 0.413).

Moreover, significant associations were found between slower processing speed (TMT A) and lower whole-brain (r = −0.16, *p* = 0.009, pFDR = 0.031), frontal (r = −0.17, *p* = 0.006, pFDR = 0.031), and temporal (r = −0.14, *p* = 0.021, pFDR = 0.049) GM/WM boundary FA_T, but not for lower processing speed with parietal (r = −0.11, *p* = 0.072, pFDR = 0.101) or occipital GM/WM boundary FA_T (r = −0.05, *p* = 0.448, pFDR = 0.448), deep WM FA_T (r = −0.12, *p* = 0.042, pFDR = 0.073), or cortical thickness (r = −0.05, *p* = 0.441, pFDR = 0.448).

Last, significant associations were found between poorer executive functioning (TMT B) and lower parietal GM/WM boundary FA_T (r = −0.17, *p* = 0.005, pFDR = 0.035), but not whole-brain (r = −0.06, *p* = 0.304, pFDR = 0.709), frontal (r = −0.02, *p* = 0.716, pFDR = 0.817), temporal (r = −0.03, *p* = 0.663, pFDR = 0.817), or occipital GM/WM boundary FA_T (r = −0.10, *p* = 0.120, pFDR = 0.420), deep WM FA_T (r = −0.01, *p* = 0.817, pFDR = 0.817), or cortical thickness (r = −0.04, *p* = 0.477, pFDR = 0.817) (Figures 3 and 4).
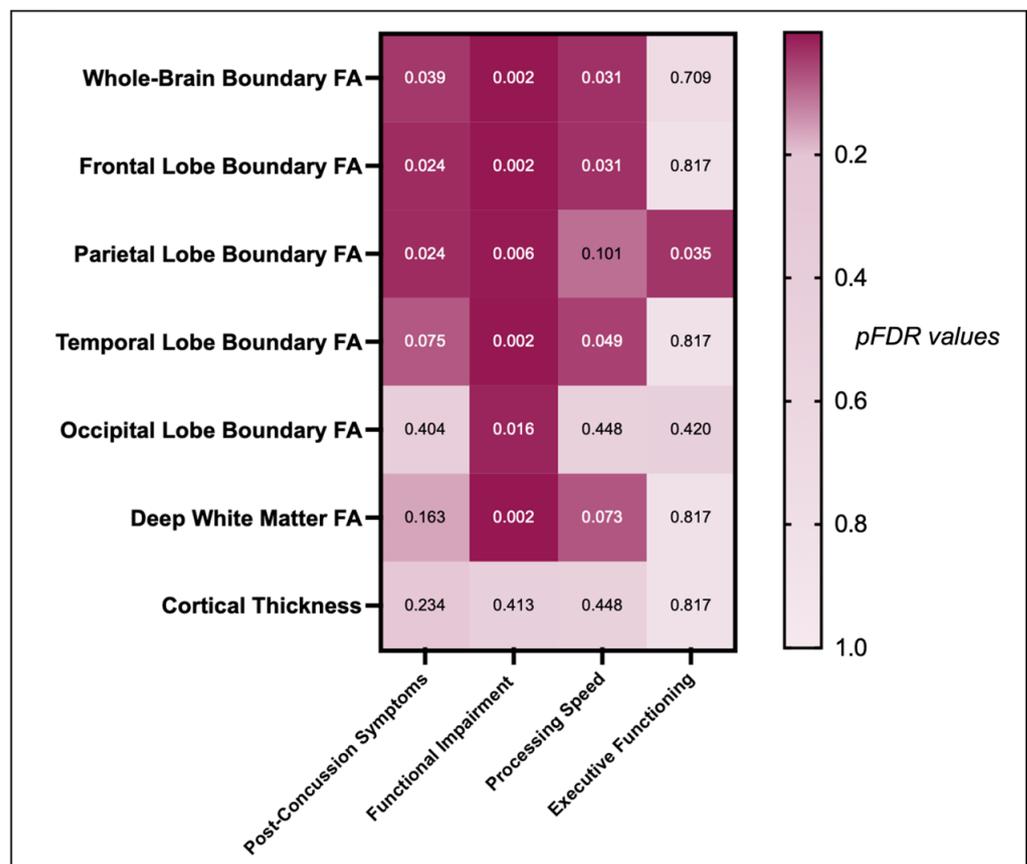
Figure 3. Association between GM/WM boundary diffusion, deep white matter, cortical thickness, and long-term outcomes (symptoms, functional impairment, processing speed, executive functioning), displayed by a heatmap of *p*FDR-values. Dark red boxes indicate a stronger relationship between imaging and outcome measures, whereas brighter boxes indicate a weak relationship between imaging and outcome measures. *Note.* FA, Fractional anisotropy.
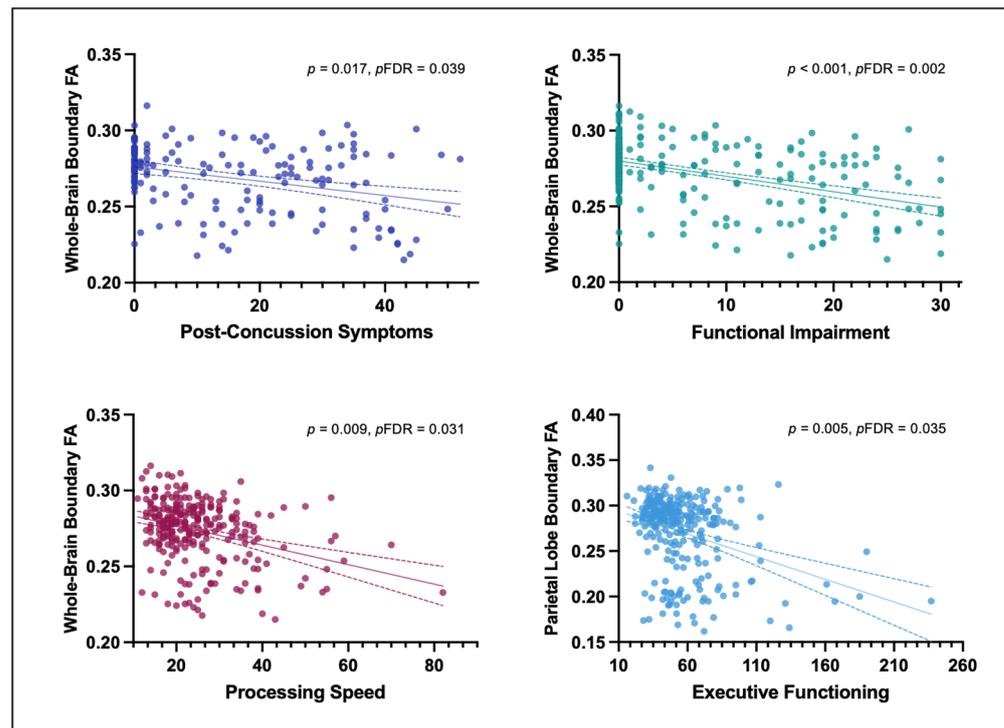
Figure 4. Associations between GM/WM boundary diffusion, post-concussive symptoms, functional impairments, and cognitive functioning. In all analyses, GM/WM boundary diffusion was negatively correlated with the outcome measure, suggesting an association between lower GM/WM diffusion and poorer long-term outcome. *Note.* FA, Fractional anisotropy; Post-Concussion Symptoms (RPQ13 Score); Functional Impairment (SDS Score); Processing Speed (TMT-A time in seconds); Executive Functioning (TMT-B time in seconds).

4. Discussion

This study found that the group with a history of mTBI (mean 7.57 ± 9.54 years after mTBI) had significantly lower whole-brain and lobe-specific GM/WM boundary FA, as well as lower deep WM FA compared to participants without mTBI. Interestingly, more severe post-concussive symptoms, slower processing speed, poorer executive functioning, and poorer functioning in work, family, and social life were significantly associated with lower GM/WM boundary FA but not with deep WM FA. There were no group differences in cortical thickness. These findings suggest that microstructural alterations at the GM/WM boundary may be a sensitive marker of adverse effects of long-term outcomes following mTBI.

4.1. WM and GM Alterations Following mTBI

The group of participants with mTBI showed lower WM FA, compared to participants without mTBI. This is in line with some previous studies that report widespread lower WM FA in individuals with a history of mTBI [15]. When acceleration and rotational forces act on the skull, the strain is transferred to the brain's tissue and may result in the tearing or shearing of axons. This shearing of axons has previously been associated with lower FA [46]. Previous research further suggest that lower FA may reflect gliosis, demyelination, and/or inflammation months to years post-injury [47].

In the current study, we also report diffusion alterations at the GM/WM boundary many years following mTBI, suggesting that shear strain at the GM/WM boundary may result in long-lasting pathology. Of interest here, a study using a computer simulation of head impact predicted that strain and strain rate are highest at the GM/WM boundary [10]. This is likely due to differences in tissue viscoelastic properties of WM compared to GM, which may increase the likelihood of shearing of GM against WM [8]. The GM/WM

boundary may thus be particularly vulnerable to shear strain-induced axonal injury and subsequently also to TAI-related pathologies [10].

4.2. Association between GM/WM Boundary Diffusion and Long-Term Outcome Following mTBI

A large percentage (46.6%) of the mTBI group exhibited post-concussive symptoms years after injury (the average time since injury was 7.57 years in this sample), which is consistent with the literature [5]. Further, more severe post-concussive symptoms were associated with lower whole-brain and lobe-specific GM/WM boundary FA. This association was still significant when adjusting for common confounders of brain structure (i.e., age, gender, PTSD, depressive symptoms, and alcohol use) suggesting that WM alterations at the GM/WM boundary may be sensitive to adverse long-term outcomes following mTBI. Of further note, we observed lower GM/WM boundary FA values in the mTBI group, particularly in older participants with greater psychiatry symptom burden, potentially suggesting additive effects.

In previous studies, lower deep WM FA post-injury has been associated with neuroinflammation, characterized by the activation of microglia, astrocytes, and the release of inflammatory cytokines, which exacerbates myelin loss, and impairs neurogenesis [47]. Altered microstructure at the GM/WM boundary may thus affect communication between brain regions that belong to functional connectivity networks [48], which have been associated with post-concussive symptoms [49]. Moreover, we hypothesize that degeneration or demyelination of axons at the GM/WM boundary may be associated with disruptions in communication between cortical and subcortical structures. Indeed, mTBI has been linked to altered functional connectivity within large-scale brain networks, such as the default mode network. Particularly intriguing, altered functional network activity has previously been observed in individuals who exhibit post-concussive symptoms [50].

In addition to an association between post-concussive symptoms and lower GM/WM boundary FA, we report an association between poorer functioning in work, family, and social life, and lower whole-brain, frontal, parietal, temporal, and occipital GM/WM boundary FA and deep WM FA. Long-term functional impairment is common after mTBI, and our results are consistent with findings that associate functional impairment with mTBI-related WM alterations [51]. Importantly, results from this study extend the current literature by suggesting that FA at the GM/WM boundary is a sensitive marker of functional impairment following mTBI.

Finally, lower whole-brain, frontal, and temporal GM/WM boundary FA were significantly correlated with slower processing speed, while lower parietal lobe GM/WM boundary FA was associated with poorer executive functioning. In this regard, mTBI has consistently been linked to reduced processing speed and impaired executive functioning [52]. In addition, effective communication across several brain areas is a prerequisite for both processing speed and executive functioning tasks [53]. The prefrontal cortex is particularly important for executive functioning, and damage to this area may result in impaired cognitive functioning that includes mental flexibility, task switching, attention, and decision making [54]. Indeed, the central executive network, a large-scale brain network that encompasses the dorsolateral prefrontal cortex and posterior parietal cortex [55], is commonly disrupted in chronic mTBI patients [50]. We speculate that by aggravating disrupted signal transmission across these cortical regions, mTBI-related injury at the GM/WM boundary may contribute to poor cognitive outcomes [56].

These findings, taken together, suggest that microstructural alterations at the GM/WM boundary may be sensitive markers of adverse long-term outcomes including processing speed, executive functioning, and functioning in work, family, and social life, following mTBI.

4.3. Limitations and Future Directions

We acknowledge several limitations in the current study. First, we analyzed cross-sectional data, precluding the inference of conclusions based on causal relationships be-

tween the study variables. Longitudinal studies are thus needed to evaluate changes in diffusion properties at the GM/WM boundary over time. Ideally, a large sample should be followed over time (i.e., pre-injury, within 24 h of injury, acutely, sub-acutely, and in the chronic stages post-injury). Further, for a comparison group, individuals with orthopedic injuries may be considered in addition to a group of uninjured individuals to mitigate bias. In addition, various imaging modalities should be correlated with neuropsychological outcomes that can be contrasted against each other to identify biomarkers of mTBI sensitive to adverse long-term outcomes. Second, the mTBI assessment was based on self-report, without available medical records or other information on injury mechanism, previous mTBI, and premorbid estimates of symptoms for validation. Third, gender, not biological sex, was assessed via the study's demographic questionnaire. Unfortunately, we lack data on how many participants identified as a gender other than their biological sex. Fourth, while participants were recruited as part of the Department of Defense INTRuST Clinical Consortium, information about military status was not available, meaning we were unable to identify a participant as a civilian or a deployed combat veteran. This is important to know since causes of military mTBI have been shown to differ from causes of civilian mTBI, given that military blast-related injuries affect brain structure and function more profoundly than blunt injuries [57]. The mechanism of injury may also likely be relevant to the GM/WM boundaries that are subjected to the most strain [10].

Last, we investigated whole-brain GM, WM, and whole-brain and lobe-specific GM/WM boundary alterations, rather than focusing on individual cortical areas or specific WM tracts. Given the lack of research on mTBI-related alterations at the GM/WM boundary, we chose this approach to provide an initial broad overview of GM/WM boundary alterations and associated clinical burden. Moreover, delineating the GM/WM boundary and transferring low-resolution and echo planar imaging (EPI) distorted diffusion data onto the anatomical space is particularly challenging in small regions of interest compared to the entire brain. Future studies will likely benefit from employing a combination of structural and functional imaging to identify network hubs and more specific brain regions and their connections, which may be vulnerable to GM/WM boundary injury and associated post-concussive burdens.

5. Conclusions

We report microstructure alterations at the GM/WM boundary in a group of individuals with a history of mTBI compared to a comparison group. Moreover, in the mTBI group, lower GM/WM boundary FA is associated with post-concussive symptom severity and poor clinical and cognitive functioning. We conclude that microstructural alterations at the GM/WM boundary may serve as a sensitive marker of mTBI-related adverse long-term outcomes following mTBI.

Institutional Review Board Statement: The study received institutional review board permission from each site's respective institutional review board, and it was carried out in accordance with the Declaration of Helsinki.

Informed Consent Statement: All study participants provided written informed consent prior to enrolment.

Data Availability Statement: The data presented in this study is available on request from the corresponding author.

Conflicts of Interest: E. Kaufmann received speaker honoraria and financial compensation for travel expenses from Medtronic, UCB, Livanova, and Eisai and has participated in clinical trials for Medtronic, UCB and Precisis, all unrelated to the submitted work. Her research is supported by the Medical Clinical Scientist Program (MCSP). M. B. Stein has received consulting income from Actelion, Acadia Pharmaceuticals, Aptinyx, atai Life Sciences, Boehringer Ingelheim, Bionomics, BioXcel Therapeutics, Eisai, Clexio, EmpowerPharm, Engrail Therapeutics, GW Pharmaceuticals, Janssen, Jazz Pharmaceuticals, and Roche/Genentech. M. B. Stein holds stock options in Oxeia Biopharmaceuticals and EpiVario. He is compensated for his work as Editor-in-Chief of *Depression and Anxiety*, Deputy Editor of *Biological Psychiatry*, and Co-Editor-in-Chief for Psychiatry of *UpToDate*. I. K. Koerte is a professor at Ludwig-Maximilians-Universität Munich (paid position). She serves as European Editor at the *Journal of Neurotrauma* (unpaid position) and as Vice President of the *European Neurotrauma Organization* (unpaid position). She receives research grant funding from the National Institutes of Health, the European Research Council, and the German Ministry for Research and Education. She receives funding for a research study on sport-related concussions from Abbott Inc. The Ludwig-Maximilians-University Hospital received donations for her research from the Schatt Foundation and from Mary Ann Liebert Inc. She receives royalties for book chapters published by Thieme Publishers. Her spouse is an employee at Siemens, and she thus holds stock options at Siemens and Siemens Healthineers. I. K. Koerte's in-kind contributions: Ph.D. students working under her supervision receive scholarships from the Villigst Foundation, the China Scholarship Council collaboration with Ludwig-Maximilians-University Munich, and Fulbright. The other authors disclose no financial or other biomedical interests or potential conflict of interest.

References

1. Lindquist, L.K.; Love, H.C.; Elbogen, E.B. Traumatic Brain Injury in Iraq and Afghanistan Veterans: New Results from a National Random Sample Study. *J. Neuropsychiatry Clin. Neurosci.* **2017**, *29*, 254–259. [CrossRef]
2. Schneiderman, A.I.; Braver, E.R.; Kang, H.K. Understanding Sequelae of Injury Mechanisms and Mild Traumatic Brain Injury Incurred during the Conflicts in Iraq and Afghanistan: Persistent Postconcussive Symptoms and Posttraumatic Stress Disorder. *Am. J. Epidemiol.* **2008**, *167*, 1446–1452. [CrossRef] [PubMed]
3. Gardner, R.C.; Yaffe, K. Epidemiology of Mild Traumatic Brain Injury and Neurodegenerative Disease. *Mol. Cell. Neurosci.* **2015**, *66*, 75–80. [CrossRef] [PubMed]
4. Maas, A.I.R.; Menon, D.K.; Manley, G.T.; Abrams, M.; Åkerlund, C.; Andelic, N.; Aries, M.; Bashford, T.; Bell, M.J.; Bodien, Y.G.; et al. Traumatic Brain Injury: Progress and Challenges in Prevention, Clinical Care, and Research. *Lancet Neurol.* **2022**, *21*, 1004–1060. [CrossRef]
5. Cancelliere, C.; Verville, L.; Stubbs, J.L.; Yu, H.; Hincapié, C.A.A.; Cassidy, J.D.; Wong, J.J.; Shearer, H.; Connell, G.; Southerst, D.; et al. Post-Concussion Symptoms and Disability in Adults with Mild Traumatic Brain Injury: A Systematic Review and Meta-Analysis. *J. Neurotrauma* **2023**, *40*, 1045–1059. [CrossRef] [PubMed]
6. Chen, Q.; Chen, X.; Xu, L.; Zhang, R.; Li, Z.; Yue, X.; Qiao, D. Traumatic Axonal Injury: Neuropathological Features, Postmortem Diagnostic Methods, and Strategies. *Forensic Sci. Med. Pathol.* **2022**, *18*, 530–544. [CrossRef]
7. Johnson, V.E.; Stewart, W.; Smith, D.H. Axonal Pathology in Traumatic Brain Injury. *Exp. Neurol.* **2013**, *246*, 35–43. [CrossRef]
8. Budday, S.; Nay, R.; de Rooij, R.; Steinmann, P.; Wyrobek, T.; Ovaert, T.C.; Kuhl, E. Mechanical Properties of Gray and White Matter Brain Tissue by Indentation. *J. Mech. Behav. Biomed. Mater.* **2015**, *46*, 318–330. [CrossRef]

9. Alisafaei, F.; Gong, Z.; Johnson, V.E.; Dollé, J.P.; Smith, D.H.; Shenoy, V.B. Mechanisms of Local Stress Amplification in Axons near the Gray-White Matter Interface. *Biophys. J.* **2020**, *119*, 1290–1300. [CrossRef]

10. Ghajari, M.; Hellyer, P.J.; Sharp, D.J. Computational Modelling of Traumatic Brain Injury Predicts the Location of Chronic Traumatic Encephalopathy Pathology. *Brain* **2017**, *140*, 333–343. [CrossRef]

11. Liu, J.; Kou, Z.F.; Tian, Y.Q. Diffuse Axonal Injury after Traumatic Cerebral Microbleeds: An Evaluation of Imaging Techniques. *Neural Regen. Res.* **2014**, *9*, 1222. [CrossRef] [PubMed]

12. Messé, A.; Caplain, S.; Pélégrini-Issac, M.; Blancho, S.; Montreuil, M.; Lévy, R.; Lehéricy, S.; Benali, H. Structural Integrity and Postconcussion Syndrome in Mild Traumatic Brain Injury Patients. *Brain Imaging Behav.* **2012**, *6*, 283–292. [CrossRef] [PubMed]

13. Oehr, L.; Anderson, J. Diffusion-Tensor Imaging Findings and Cognitive Function Following Hospitalized Mixed-Mechanism Mild Traumatic Brain Injury: A Systematic Review and Meta-Analysis. *Arch. Phys. Med. Rehabil.* **2017**, *98*, 2308–2319. [CrossRef]

14. Shenton, M.E.; Hamoda, H.M.; Schneiderman, J.S.; Bouix, S.; Pasternak, O.; Rathi, Y.; Vu, M.A.; Purohit, M.P.; Helmer, K.; Koerte, I.; et al. A Review of Magnetic Resonance Imaging and Diffusion Tensor Imaging Findings in Mild Traumatic Brain Injury. *Brain Imaging Behav.* **2012**, *6*, 137–192. [CrossRef] [PubMed]

15. Kim, E.; Yoo, R.E.; Seong, M.Y.; Oh, B.M. A Systematic Review and Data Synthesis of Longitudinal Changes in White Matter Integrity after Mild Traumatic Brain Injury Assessed by Diffusion Tensor Imaging in Adults. *Eur. J. Radiol.* **2022**, *147*, 110117. [CrossRef]

16. Lippa, S.M.; Yeh, P.-H.; Ollinger, J.; Brickell, T.A.; French, L.M.; Lange, R.T. White Matter Integrity Relates to Cognition in Service Members and Veterans after Complicated Mild, Moderate, and Severe Traumatic Brain Injury, But Not Uncomplicated Mild Traumatic Brain Injury. *J. Neurotrauma* **2022**. [CrossRef]

17. Govindarajan, K.A.; Narayana, P.A.; Hasan, K.M.; Wilde, E.A.; Levin, H.S.; Hunter, J.V.; Miller, E.R.; Patel, V.K.S.; Robertson, C.S.; McCarthy, J.J. Cortical Thickness in Mild Traumatic Brain Injury. *J. Neurotrauma* **2016**, *33*, 1809–1817. [CrossRef]

18. España, L.Y.; Lee, R.M.; Ling, J.M.; Jeromin, A.; Mayer, A.R.; Meier, T.B. Serial Assessment of Gray Matter Abnormalities after Sport-Related Concussion. *J. Neurotrauma* **2017**, *34*, 3143–3152. [CrossRef]

19. Urban, K.J.; Riggs, L.; Wells, G.D.; Keightley, M.; Chen, J.K.; Ptito, A.; Fait, P.; Taha, T.; Sinopoli, K.J. Cortical Thickness Changes and Their Relationship to Dual-Task Performance Following Mild Traumatic Brain Injury in Youth. *J. Neurotrauma* **2017**, *34*, 816–823. [CrossRef]

20. Dall'Acqua, P.; Johannes, S.; Mica, L.; Simmen, H.P.; Glaab, R.; Fandino, J.; Schwendinger, M.; Meier, C.; Ulbrich, E.J.; Müller, A.; et al. Prefrontal Cortical Thickening after Mild Traumatic Brain Injury: A One-Year Magnetic Resonance Imaging Study. *J. Neurotrauma* **2017**, *34*, 3270–3279. [CrossRef]

21. Trotter, B.B.; Robinson, M.E.; Milberg, W.P.; McGlinchey, R.E.; Salat, D.H. Military Blast Exposure, Ageing and White Matter Integrity. *Brain* **2015**, *138*, 2278–2292. [CrossRef]

22. Mac Donald, C.L.; Barber, J.; Andre, J.; Panks, C.; Zalewski, K.; Temkin, N. Longitudinal Neuroimaging Following Combat Concussion: Sub-Acute, 1 Year and 5 Years Post-Injury. *Brain Commun.* **2019**, *1*, fcz031. [CrossRef] [PubMed]

23. Lange, R.T.; Yeh, P.H.; Brickell, T.A.; Lippa, S.M.; French, L.M. Postconcussion Symptom Reporting Is Not Associated with Diffusion Tensor Imaging Findings in the Subacute to Chronic Phase of Recovery in Military Service Members Following Mild Traumatic Brain Injury. *J. Clin. Exp. Neuropsychol.* **2019**, *41*, 497–511. [CrossRef] [PubMed]

24. Zivanovic, N.; Virani, S.; Rajaram, A.A.; Lebel, C.; Yeates, K.O.; Brooks, B.L. Cortical Volume and Thickness in Youth Several Years After Concussion. *J. Child. Neurol.* **2021**, *36*, 186–194. [CrossRef]

25. Mild Traumatic Brain Injury Committee, American Congress of Rehabilitation Medicine, Head Injury Interdisciplinary Special Interest Group. Definition of Mild Traumatic Brain Injury. *J. Head. Trauma Rehabil.* **1993**, *8*, 86–87. [CrossRef]

26. Umminger, L.F.; Rojczyk, P.; Seitz-Holland, J.; Sollmann, N.; Kaufmann, E.; Kinzel, P.; Zhang, F.; Kochsiek, J.; Langhein, M.; Kim, C.L.; et al. White Matter Microstructure Is Associated with Serum Neuroactive Steroids and Psychological Functioning. *J. Neurotrauma* **2022**. [CrossRef]

27. King, N.S.; Crawford, S.; Wenden, F.J.; Moss, N.E.G.; Wade, D.T. The Rivermead Post Concussion Symptoms Questionnaire: A Measure of Symptoms Commonly Experienced after Head Injury and Its Reliability. *J. Neurol.* **1995**, *242*, 587–592. [CrossRef]

28. Eyres, S.; Carey, A.; Gilworth, G.; Neumann, V.; Tennant, A. Construct Validity and Reliability of the Rivermead Post-Concussion Symptoms Questionnaire. *Clin. Rehabil.* **2005**, *19*, 878–887. [CrossRef] [PubMed]

29. Sheehan, D.V.; Harnett-Sheehan, K.; Raj, B.A. The Measurement of Disability. *Int. Clin. Psychopharmacol.* **1996**, *11* (Suppl. 3), 89–95. [CrossRef]

30. Reitan, R.M. An Investigation of the Validity of Halstead's Measures of Biological Intelligence. *Arch. Neurol. Psychiatry* **1955**, *73*, 28–35. [CrossRef]

31. Stuss, D.T.; Stethem, L.L.; Hugenholtz, H.; Richard, M.T. Traumatic Brain Injury: A Comparison of Three Clinical Tests, and Analysis of Recovery. *Clin. Neuropsychol.* **1989**, *3*, 145–156. [CrossRef]

32. Weathers, F.W.; Litz, B.T.; Herman, D.S.; Huska, J.A.; Keane, T.M. The PTSD Checklist (PCL): Reliability, Validity, and Diagnostic Utility. In Proceedings of the Annual Conference of the International Society for Traumatic Stress Studies, San Antonio, TX, USA, 24 October 1993.

33. Kroenke, K.; Spitzer, R.L.; Williams, J.B.W. The PHQ-9: Validity of a Brief Depression Severity Measure. *J. Gen. Intern. Med.* **2001**, *16*, 606–613. [CrossRef] [PubMed]

34. Saunders, J.B.; Aasland, O.G.; Amundsen, A.; Grant, M. Alcohol Consumption and Related Problems among Primary Health Care Patients: WHO Collaborative Project on Early Detection of Persons with Harmful Alcohol Consumption—I. *Addiction* **1993**, *88*, 349–362. [CrossRef] [PubMed]

35. Fedorov, A.; Beichel, R.; Kalpathy-Cramer, J.; Finet, J.; Fillion-Robin, J.C.; Pujol, S.; Bauer, C.; Jennings, D.; Fennessy, F.; Sonka, M.; et al. 3D Slicer as an Image Computing Platform for the Quantitative Imaging Network. *Magn. Reson. Imaging* **2012**, *30*, 1323–1341. [CrossRef] [PubMed]

36. Fischl, B. FreeSurfer. *Neuroimage* **2012**, *62*, 774–781. [CrossRef]

37. Destrieux, C.; Fischl, B.; Dale, A.; Halgren, E. Automatic Parcellation of Human Cortical Gyri and Sulci Using Standard Anatomical Nomenclature. *Neuroimage* **2010**, *53*, 1–15. [CrossRef]

38. Fischl, B.; Dale, A.M. Measuring the Thickness of the Human Cerebral Cortex from Magnetic Resonance Images. *Proc. Natl. Acad. Sci. USA* **2000**, *97*, 11050–11055. [CrossRef]

39. Mirzaalian, H.; Ning, L.; Savadjiev, P.; Pasternak, O.; Bouix, S.; Michailovich, O.; Grant, G.; Marx, C.E.; Morey, R.A.; Flashman, L.A.; et al. Inter-Site and Inter-Scanner Diffusion MRI Data Harmonization. *Neuroimage* **2016**, *135*, 311–323. [CrossRef]

40. Chien, D.; Buxton, R.B.; Kwong, K.K.; Brady, T.J.; Rosen, B.R. MR Diffusion Imaging of the Human Brain. *J. Comput. Assist. Tomogr.* **1990**, *14*, 514–520. [CrossRef]

41. Pasternak, O.; Sochen, N.; Gur, Y.; Intrator, N.; Assaf, Y. Free Water Elimination and Mapping from Diffusion MRI. *Magn. Reson. Med.* **2009**, *62*, 717–730. [CrossRef]

42. Smith, S.M.; Jenkinson, M.; Johansen-Berg, H.; Rueckert, D.; Nichols, T.E.; Mackay, C.E.; Watkins, K.E.; Ciccarelli, O.; Cader, M.Z.; Matthews, P.M.; et al. Tract-Based Spatial Statistics: Voxelwise Analysis of Multi-Subject Diffusion Data. *Neuroimage* **2006**, *31*, 1487–1505. [CrossRef] [PubMed]

43. Jahanshad, N.; Kochunov, P.v.; Sprooten, E.; Mandl, R.C.; Nichols, T.E.; Almasy, L.; Blangero, J.; Brouwer, R.M.; Curran, J.E.; de Zubicaray, G.I.; et al. Multi-Site Genetic Analysis of Diffusion Images and Voxelwise Heritability Analysis: A Pilot Project of the ENIGMA-DTI Working Group. *Neuroimage* **2013**, *81*, 455–469. [CrossRef] [PubMed]

44. Greve, D.N.; Fischl, B. Accurate and Robust Brain Image Alignment Using Boundary-Based Registration. *Neuroimage* **2009**, *48*, 63–72. [CrossRef] [PubMed]

45. Hochberg, Y.; Benjamini, Y. More Powerful Procedures for Multiple Significance Testing. *Stat. Med.* **1990**, *9*, 811–818. [CrossRef]

46. Donat, C.K.; Yanez Lopez, M.; Sastre, M.; Baxan, N.; Goldfinger, M.; Seeamber, R.; Müller, F.; Davies, P.; Hellyer, P.; Siegkas, P.; et al. From Biomechanics to Pathology: Predicting Axonal Injury from Patterns of Strain after Traumatic Brain Injury. *Brain* **2021**, *144*, 70–91. [CrossRef]

47. Simon, D.W.; McGeachy, M.J.; Baylr, H.; Clark, R.S.B.; Loane, D.J.; Kochanek, P.M. The Far-Reaching Scope of Neuroinflammation after Traumatic Brain Injury. *Nat. Rev. Neurol.* **2017**, *13*, 171–191. [CrossRef]

48. Cramer, S.W.; Haley, S.P.; Popa, L.S.; Carter, R.E.; Scott, E.; Flaherty, E.B.; Dominguez, J.; Aronson, J.D.; Sabal, L.; Surinach, D.; et al. Wide-Field Calcium Imaging Reveals Widespread Changes in Cortical Functional Connectivity Following Mild Traumatic Brain Injury in the Mouse. *Neurobiol. Dis.* **2023**, *176*, 105943. [CrossRef]

49. Hocke, L.M.; Duszynski, C.C.; Debert, C.T.; Dleikan, D.; Dunn, J.F. Reduced Functional Connectivity in Adults with Persistent Post-Concussion Symptoms: A Functional Near-Infrared Spectroscopy Study. *J. Neurotrauma* **2018**, *35*, 1224–1232. [CrossRef]

50. D'Souza, M.M.; Kumar, M.; Choudhary, A.; Kaur, P.; Kumar, P.; Rana, P.; Trivedi, R.; Sekhri, T.; Singh, A.K. Alterations of Connectivity Patterns in Functional Brain Networks in Patients with Mild Traumatic Brain Injury: A Longitudinal Resting-State Functional Magnetic Resonance Imaging Study. *Neuroradiol. J.* **2020**, *33*, 186–197. [CrossRef]

51. Mohammadian, M.; Roine, T.; Hirvonen, J.; Kurki, T.; Posti, J.P.; Katila, A.J.; Takala, R.S.K.; Tallus, J.; Maanpää, H.R.; Frantzén, J.; et al. Alterations in Microstructure and Local Fiber Orientation of White Matter Are Associated with Outcome after Mild Traumatic Brain Injury. *J. Neurotrauma* **2020**, *37*, 2616–2623. [CrossRef]

52. Gaines, K.D.; Soper, H.v.; Berenji, G.R. Executive Functioning of Combat Mild Traumatic Brain Injury. *Appl. Neuropsychol. Adult* **2016**, *23*, 115–124. [CrossRef]

53. Bullmore, E.; Sporns, O. The Economy of Brain Network Organization. *Nat. Rev. Neurosci.* **2012**, *13*, 336–349. [CrossRef] [PubMed]

54. Cristofori, I.; Cohen-Zimerman, S.; Grafman, J. Executive Functions. *Handb. Clin. Neurol.* **2019**, *163*, 197–219. [CrossRef] [PubMed]

55. Menon, V. Large-Scale Brain Networks and Psychopathology: A Unifying Triple Network Model. *Trends Cogn. Sci.* **2011**, *15*, 483–506. [CrossRef]

56. Cristofori, I.; Zhong, W.; Chau, A.; Solomon, J.; Krueger, F.; Grafman, J. White and Gray Matter Contributions to Executive Function Recovery after Traumatic Brain Injury. *Neurology* **2015**, *84*, 1394. [CrossRef] [PubMed]

57. Przekwas, A.; Garimella, H.T.; Tan, X.G.; Chen, Z.J.; Miao, Y.; Harrand, V.; Kraft, R.H.; Gupta, R.K. Biomechanics of Blast TBI With Time-Resolved Consecutive Primary, Secondary, and Tertiary Loads. *Mil. Med.* **2019**, *184*, 195–205. [CrossRef]